Kinetics and Thermodynamics of the Gas Phase Reaction $SO_3 + NH_3 + N_2 \leftrightarrow H_3NSO_3 + N_2$

Edward R. Lovejoy

NOAA Aeronomy Laboratory, 325 Broadway, Boulder, Colorado 80303

Received: February 24, 1997; In Final Form: April 15, 1997[⊗]

The kinetics of the gas phase reaction $SO_3 + NH_3 + N_2 \leftrightarrow H_3NSO_3 + N_2$ were studied with a flow reactor coupled to a chemical ionization mass spectrometer for detection of SO_3 and H_3NSO_3. The rate coefficient for the association reaction $SO_3 + NH_3 + N_2$ was measured as a function of temperature (280−340 K) and pressure (20−80 Torr of N_2). Analysis of the SO_3 decay and H_3NSO_3 appearance at higher temperatures yielded rate coefficients for H_3NSO_3 decomposition and the enthalpy of the reaction $SO_3 + NH_3 \leftrightarrow H_3NSO_3$: $\Delta H^\circ_{298K} = -24 \pm 1$ kcal mol^{-1}.

Introduction

The dominant loss mechanism for SO_3 in the atmosphere is reaction with gas phase water to produce sulfuric acid.[1−3] The association reaction of SO_3 with ammonia (eq 1) typically

$$SO_3 + NH_3 + M \leftrightarrow H_3NSO_3 + M \qquad (1)$$

accounts for less than 10^{-4} of the SO_3 loss in the atmosphere.[3,4] H_3NSO_3 appears to have an unusually strong affinity for H_2SO_4, and it has been proposed that the association of H_3NSO_3 and H_2SO_4 may be an important step in the formation of aerosol in the atmosphere despite the low concentrations of H_3NSO_3.[4]

The stability of H_3NSO_3 is not well established. High-level calculations by Wong et al. predict that H_3NSO_3 is bound by about 19 kcal mol^{-1} relative to NH_3 and SO_3.[5] Lovejoy and Hanson[4] report that the H_3N-SO_3 bond enthalpy is greater than 20 kcal mol^{-1}, based on the observation of exponential SO_3 decays in excess NH_3 at room temperature.

The theoretical work by Wong et al.[5] predicts that gas phase H_3NSO_3 is a zwitterion with significant electron donation from the N to S leading to a large dipole moment of 6.6 D. Wong et al.[5] also predict that gas phase H_3NSO_3 has a significantly longer (about 0.1 Å) N−S bond than the solid form. Canagaratna et al.[6] have measured the microwave spectrum of gas phase H_3NSO_3 and find that the structure agrees very well with the theoretical predictions of Wong et al.[5] They also confirm that H_3NSO_3 is a zwitterion with about 0.4 electrons transferred from N to S.

Shen et al.[7] reported the first kinetic measurements for the reaction $SO_3 + NH_3$. They measured a rate coefficient of $(6.9 \pm 1.5) \times 10^{-11}$ cm^3 molecule^{-1} s^{-1} in 1−2 Torr of He with a flow reactor and photofragment-emission detection of SO_3. Lovejoy and Hanson[4] have recently reported measurements of the pressure dependence of the association rate coefficient and observation of the H_3NSO_3 product.

In the present work, the kinetics of the loss of SO_3 in the presence of NH_3 are measured as a function of temperature (280−343 K) and pressure (20−80 Torr of N_2). At elevated temperatures (383−402 K) the decomposition of H_3NSO_3 is observed, and equilibrium constants for reaction 1 are measured. These data yield the temperature dependence of the $SO_3 + NH_3$ reaction near the low-pressure limit and the heat of formation of H_3NSO_3. The implications of these results to the understanding of the atmospheric chemistry of H_3NSO_3 are discussed.

Experimental Section

The kinetics of the reaction of SO_3 with NH_3 were studied by monitoring the concentration of SO_3 at the exit of a laminar flow reactor as a function of the contact distance between SO_3 and NH_3. SO_3 was monitored with chemical ionization mass spectrometry.[3] The reactor was a Pyrex cylinder 50 cm long with a 1.62 cm internal diameter. The temperature of the reactor was controlled by circulating temperature-regulated fluid through copper tubing soldered to an insulated copper sleeve surrounding the reactor. The reactor temperature was measured with a thermocouple mounted on the end of a movable inlet. The temperature gradient was less than 2 K along the reaction zone for the conditions of the present work. SO_3 was generated near the end of the movable inlet by oxidizing SO_2 on a hot nichrome filament in the presence of O_2, as described previously.[3] Ammonia was added to the reactor at the upstream end along with the main flow of N_2. Mixtures of NH_3 in N_2 were prepared in 12 L Pyrex bulbs by adding measured pressures of NH_3 and N_2. The reactor pressure was measured with a capacitance manometer and gas flows were measured with mass flow meters. The mass flow meters were calibrated with a wet test meter or by measuring the rate of change of pressure in a calibrated volume.

The CIMS ion−molecule reactor was operated at 5 Torr with about a 0.1 s contact time with the SO_3 reactor effluent. SO_3 was detected by using the following reactions[3,8]

$$NO_3^-HNO_3 + SO_3 \rightarrow NO_3^-SO_3 + HNO_3 \qquad (2)$$

and

$$SiF_5^- + SO_3 \rightarrow FSO_3^- + SiF_4 \qquad (3)$$

H_3NSO_3 was detected by using

$$NO_3^-HNO_3 + H_3NSO_3 \rightarrow H_2NSO_3^-HNO_3 + HNO_3 \qquad (4)$$

Initial SO_3 concentrations in the neutral flow reactor ranged from about $(1-10) \times 10^9$ molecule cm^{-3}. The NH_3 concentration was typically at least 50 times larger than $[SO_3]$ so that

[⊗] Abstract published in *Advance ACS Abstracts,* June 15, 1997.

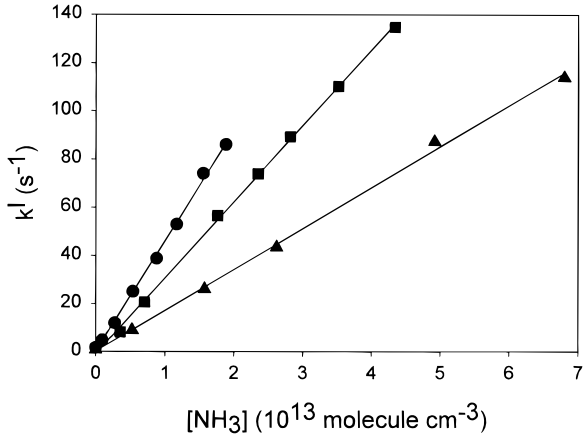

Figure 1. First-order rate coefficient for SO_3 loss as a function of $[NH_3]$ and temperature. Circles = 280 K, 41.4 Torr. Squares = 301 K, 41.0 Torr. Triangles = 334 K, 40.6 Torr.

TABLE 1: Summary of $SO_3 + NH_3$ Rate Coefficients

$p(N_2)$ (Torr)	T (K)	v^a (cm s^{-1})	$[NH_3]_{max}$ (10^{12} molecules cm^{-3})	no. of k^I measmnts	k_f^b (10^{-12} cm^3 molecule^{-1} s^{-1})
20.5	280	391	53	7	2.76 (0.06)
20.1	298	423	81	8	1.90 (0.10)
21.1	317	445	124	9	1.34 (0.14)
20.2	317	441	118	6	1.35[c] (0.08)
20.5	341	472	133	8	0.87[c] (0.05)
41.4	280	197	19	8	4.58 (0.16)
41.0	301	214	43	8	3.16 (0.06)
41.0	319	237	72	7	2.30 (0.14)
40.6	334	240	68	6	1.70 (0.08)
40.0	343	247	88	6	1.47 (0.10)
81.3	280	100	4.9	6	8.2 (0.3)
79.8	300	107	7.1	7	5.04 (0.34)
80.4	320	113	13	8	3.47 (0.22)

[a] Average reactor flow velocity. [b] 95% confidence levels for precision are indicated in parentheses. [c] SiF_5^- reagent ion.

the SO_3 loss was pseudo first order in SO_3. The Reynolds number for the neutral reactor flow was about 75.

Results and Discussion

Rate coefficients were measured by monitoring the concentration of SO_3 at the exit of the flow reactor as a function of the contact distance with NH_3 for a range of NH_3 concentrations. The $NO_3^-HNO_3$ reagent ion was used for the majority of the measurements. At temperatures below 350 K the SO_3 decays were exponential, as expected for a first-order process, and as observed previously.[4] First-order SO_3 loss rate coefficients were extracted from the decays by using the Brown algorithm.[9] First-order rate coefficients are plotted as a function of the concentration of NH_3 for a range of temperatures in 40 Torr of N_2 in Figure 1. The slopes of these plots yield the effective second-order rate coefficients for $SO_3 + NH_3$. All of the measured association rate coefficients are listed in Table 1. The quoted errors are the 95% confidence levels for precision only. The overall uncertainty in the rate coefficients is estimated to be ±20%. The room temperature rate coefficients measured in this work are in excellent agreement with the previous measurements of Lovejoy and Hanson,[4] but are about 100 times smaller than the original measurement by Shen et al.[7] Heterogeneous loss of SO_3, possibly related to the relatively high levels of SO_3, may have influenced the Shen et al.[7] measurement.

The pressure and temperature dependence of the rate coefficient for a three-body reaction may be described by the Troe formalism[10]

$$k(M, T) = \left(\frac{k_0(T)[M]}{1 + \frac{k_0(T)[M]}{k_\infty(T)}}\right)0.6^y \quad (5)$$

$$y = \left(1 + \left[\log\left(\frac{k_0(T)[M]}{k_\infty(T)}\right)\right]^2\right)^{-1}$$

where $k_0(T) = k_0^{300}(T/300)^{-n}$ and $k_\infty(T) = k_\infty^{300}(T/300)^{-m}$. A fit of the $k(M,T)$ data (Table 1) to eq 5, including the previous measurements[4] at 295 K, gives $k_0^{300} = (3.6 \pm 0.4) \times 10^{-30}$ cm^6 molecule^{-2} s^{-1}, $k_\infty^{300} = (4.3 \pm 1.2) \times 10^{-11}$ cm^3 molecule^{-1} s^{-1}, and $n = 6.1 \pm 1.0$, with m fixed equal to zero. The errors reflect an estimated 20% uncertainty in the measured rate coefficients. The fit results changed by less than 10% for $0 < m < 3$. The assumption that the high-pressure limiting rate coefficient is independent of temperature (i.e. $m = 0$) is reasonable considering that the high-pressure limit rate coefficient is large at room temperature and the temperature dependence of k_∞ is generally weak (see, for example, ref 10).

At temperatures above 380 K the unimolecular decomposition of H_3NSO_3 into $SO_3 + NH_3$ competed efficiently with the association reaction, and the SO_3 decays were not simple exponentials (see Figure 2). For these conditions the SO_3 decay and H_3NSO_3 appearance were modeled to extract the rate coefficient for decomposition of H_3NSO_3. The kinetics were modeled with the following mechanism

$$SO_3 + NH_3 + M \leftrightarrow H_3NSO_3 + M \qquad (k_f, k_r) \quad (6)$$

$$SO_3 + \text{wall} \rightarrow \qquad (k_w^{SO_3}) \quad (7)$$

$$H_3NSO_3 + \text{wall} \rightarrow \qquad (k_w^{SA}) \quad (8)$$

For this mechanism $[SO_3]$ and $[H_3NSO_3]$ are described by

$$[SO_3] = \frac{[SO_3]_0}{a - b}[(a + c)\exp(at) - (b + c)\exp(bt)] \quad (9)$$

and

$$[H_3NSO_3] = \frac{k_f[NH_3][SO_3]_0}{a - b}[\exp(at) - \exp(bt)] \quad (10)$$

where

$$a = 0.5[(d^2 - 4e)^{1/2} - d]$$

$$b = -0.5[(d^2 - 4e)^{1/2} + d]$$

$$c = k_r + k_w^{SA}$$

$$d = k_f[NH_3] + k_r + k_w^{SO3} + k_w^{SA}$$

$$e = k_w^{SA}k_f[NH_3] + k_rk_w^{SO3} + k_w^{SA}k_w^{SO3}$$

The SO_3 decay and H_3NSO_3 appearance were fit simultaneously to these equations with k_f fixed at the value extrapolated from the lower temperature data. The reaction time was calculated using the relationship $t = z/(1.7v)$ where z is the reaction distance and v is the average flow velocity.[4] The rate coefficient for SO_3 wall loss was fixed at the value measured in the absence of NH_3. This value was always within 10% of the diffusion-limited value, implying that the SO_3 reaction probability with the reactor wall was greater than 10^{-3}. The nonlinear regression variables included the first-order H_3NSO_3

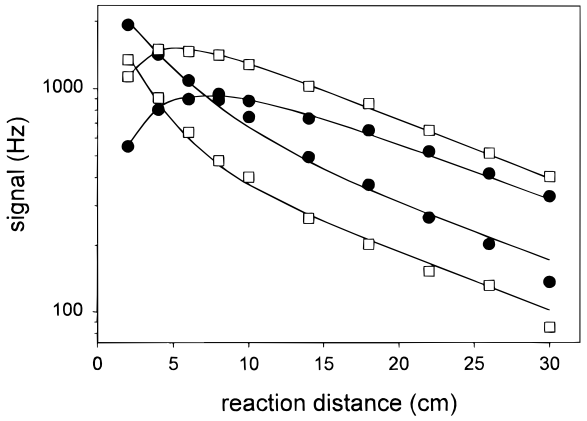

Figure 2. SO_3 and H_3NSO_3 signals ($NO_3^-SO_3$ and $H_2NSO_3^-HNO_3$) as a function of reaction distance and $[NH_3]$. Reactor conditions: $v =$ 288 cm s^{-1}, 393 K, 40.0 Torr of N_2. Squares: $[NH_3] = 9 \times 10^{13}$ molecule cm^{-3}. Circles: $[NH_3] = 1.8 \times 10^{14}$ molecule cm^{-3}. Solid lines are fits to the data as described in the text. Fit results are listed in Table 2.

TABLE 2: Summary of $SO_3 + NH_3 + N_2 \leftrightarrow H_3NSO_3 + N_2$ Equilibrium Measurements

$p(N_2)$ (Torr)	T (K)	k_f (10^{-13} cm^3 molecule^{-1} s^{-1})	$[NH_3]$ (10^{13} molecule cm^{-3})	v (cm s^{-1})	k_r (s^{-1})	$\Delta H°$ (kcal mol^{-1})
40.8	393	7.4	5	281	44	−24.0
40.8	393	7.4	9	281	41	−24.1
40.8	393	7.4	18	281	38	−24.1
40.4	402	6.5	12	295	97	−23.8
40.4	402	6.5	12	295	94	−23.9
40.4	402	6.5	25	295	117	−23.7
40.0	393	7.3	18	288	41	−24.1
40.0	393	7.3	9	288	37	−24.2
40.3	383	8.3	9	279	22	−24.1
40.3	383	8.3	6	279	20	−24.1
40.3	383	8.3	2	279	21	−24.1
40.6	393	7.4	10	280	33	−24.3
40.6	393	7.4	14	280	38	−24.1
40.6	393	7.4	19	280	39	−24.1
40.6	393	7.4	13	280	40	−24.1
79.1	383	13	9	138	33	−24.1
79.1	383	13	19	138	48	−23.8
79.1	383	13	5	138	35	−24.0
79.1	383	13	14	138	47	−23.8
41.0	393	7.4	9	272	36	−24.2
41.0	393	7.4	14	272	41	−24.1
41.0	393	7.4	5	272	35	−24.2

decomposition rate coefficient k_r, the H_3NSO_3 wall loss (k_w^{SA}), and the CIMS sensitivity for SO_3 relative to H_3NSO_3. A set of experimental SO_3 and H_3NSO_3 profiles and the simultaneous fits to eqs 9 and 10 are presented in Figure 2. All the equilibrium measurements are summarized in Table 2. The rate coefficient for wall loss of H_3NSO_3 was consistently about 40% less than the diffusion-limited value, implying that at these elevated temperatures the wall reaction probability for H_3NSO_3 was reduced and/or evaporation of H_3NSO_3 was important. The fitted wall loss rate coefficients for H_3NSO_3 varied by less than about 20% for the range of NH_3 concentrations used in this work. The CIMS sensitivities for H_3NSO_3 and SO_3 were a function of the concentration of HNO_3 in the ion−molecule reactor. For the conditions of the present work, the CIMS was typically 1−3 times more sensitive to H_3NSO_3 than SO_3.

The equilibrium constant could only be measured over a limited range of temperatures because of the very strong temperature dependence of the rate coefficient for decomposition of H_3NSO_3. Therefore, the reaction enthalpy was derived by using a third-law analysis. The entropy of H_3NSO_3 was calculated from experimental[6] and theoretical[5] structural parameters and scaled vibrational frequencies.[5] The entropies of SO_3 and NH_3 were taken from the literature.[11] These values yielded an entropy change for the formation of H_3NSO_3 (reaction 1) of −0.036 kcal mol^{-1} K^{-1} for 250 K < T < 400 K. Calculations also showed that the change in heat capacity for reaction 1 is negligible for 300 K < T < 400 K ($|\Delta C_p| < 1$ cal mol^{-1} K^{-1}), so that $\Delta H°$ is essentially independent of temperature between 300 and 400 K.

TABLE 3: Predicted H_3NSO_3 Decomposition Lifetimes for Tropospheric Conditions

pressure (Torr)	T^a (K)	k_f (10^{-11} cm^3 molecule^{-1} s^{-1})	k_r (s^{-1})	H_3NSO_3 decomp lifetime (s)
760	281	2.2	9×10^{-3}	110
405	254	2.3	1.1×10^{-4}	9100
195	222	2.5	1.4×10^{-7}	7×10^6

[a] On the basis of a model atmosphere for 40° N in March (ref 15).

In the equilibrium experiments, data were taken in the entrance and mixing region immediately downstream of the SO_3 moveable source (see Figure 2). It should be noted that at lower temperatures SO_3 decays were linear in this region, even though the radial velocity and concentration gradients are not expected to be fully developed until about 5−10 cm downstream of the inlet.[12] On the basis of the poorly defined reaction time at short reaction distances, the uncertainties in the measured equilibrium constants are estimated to be about a factor of 2. This yields a reaction enthalpy for $SO_3 + NH_3 \leftrightarrow H_3NSO_3$ of $\Delta H°_{298K} = -24 \pm 1$ kcal mol^{-1} and a heat of formation for H_3NSO_3 of $\Delta H°_{f,298K} = -129.6 \pm 1.0$ kcal mol^{-1}, where the standard state is 1 atm. This experimental H_3N-SO_3 bond enthalpy is about 4 kcal mol^{-1} larger than the theoretical value.[5]

Atmospheric Implications

The lifetime of H_3NSO_3 with respect to unimolecular decomposition for several conditions of pressure and temperature characteristic of the troposphere are listed in Table 3. Other potential atmospheric loss processes for H_3NSO_3 include scavenging by aerosol and clustering with H_2SO_4. The heterogeneous reaction probability for H_3NSO_3 is probably near unity. In this case the lifetime of H_3NSO_3 with respect to aerosol scavenging will range from seconds in clouds to many hours in clean air.[13] Assuming a very efficient reaction with H_2SO_4[4] and ambient $[H_2SO_4]$ ranging from 10^6 to 10^7 molecule cm^{-3},[14] yields a lifetime of H_3NSO_3 with respect to clustering with H_2SO_4 of about 10^3-10^4 s. This analysis shows that the unimolecular decomposition of H_3NSO_3 is most important in the lower troposphere for clean conditions. In the free troposphere the dominant loss processes for H_3NSO_3 are probably scavenging by aerosol and clustering with H_2SO_4. In order to understand the role of H_3NSO_3 in the nucleation of atmospheric particles, the kinetics of production and decomposition of clusters of the form $H_3NSO_3(H_2SO_4)_x$ are needed.

Acknowledgment. This work was supported in part by the NOAA Climate and Global Change Program.

References and Notes

(1) Reiner, T.; Arnold, F. *J. Chem. Phys*. **1994**, *101*, 7399.
(2) Kolb, C. E.; Jayne, J. T.; Worsnop, D. R.; Molina, M. J.; Meads, R. F.; Viggiano, A. A. *J. Am. Chem. Soc*. **1994**, *116*, 10314.
(3) Lovejoy, E. R.; Hanson, D. R.; Huey, L. G. *J. Phys. Chem*. **1996**, *100*, 19911.
(4) Lovejoy, E. R.; Hanson, D. R. *J. Phys. Chem*. **1996**, *100*, 4465.
(5) Wong, M. W.; Wiberg, K. B.; Frisch, M. J. *J. Am. Chem. Soc*. **1992**, *114*, 523.

(6) Canagaratna, M.; Phillips, J. A.; Goodfriend, H.; Leopold, K. R. *J. Am. Chem. Soc.* **1996**, *118*, 5290.
(7) Shen, G.; Suto, M.; Lee, L. C. *J. Geophys. Res.* **1990**, *95*, 13981.
(8) Arnold, S. T.; Morris, R. A.; Viggiano, A. A.; Jayne, J. T. *J. Geophys. Res.* **1995**, *100*, 14141.
(9) Brown, R. L. *J. Res. Natl. Bur. Stand.* **1978**, *83*, 1.
(10) DeMore, W. B.; Sander, S. P.; Golden, D. M.; Hampson, R. F.; Kurylo, M. J.; Howard, C. J.; Ravishankara, A. R.; Kolb, C. E.; Molina, M. J. *Chemical Kinetics and Data for Use in Stratopheric Modeling*; JPL publication 94-26; Jet Propulsion Laboratory: Pasadena, CA, 1994.
(11) Chase, M. W., Jr.; Davies, C. A.; Downey, J. R., Jr.; Frurip, D. J.; McDonald, R. A.; Syverud, A. N. JANAF Thermochemical Tables. *J. Phys. Chem. Ref. Data Suppl. 1* **1985**, 14.
(12) Keyser, L. F. *J. Phys. Chem.* **1984**, *88*, 4750.
(13) Lovejoy, E. R.; Huey, L. G.; Hanson, D. R. *J. Geophys. Res*. **1995**, *100*, 18775.
(14) Weber, R. J.; McMurry, P. H.; Eisele, F. L.; Tanner, D. J. *J. Atmos. Sci.* **1995**, *52*, 2242.
(15) Houghton, J. T. *The Physics of Atmospheres*; Cambridge University Press: Cambridge, 1986.